where $\beta$ is the fermion magnetic moment and $N$ is the atomic density. The critical temperatures $T_c^{(1)}$ for magnetic transitions from the disordered phase can also be found thermodynamically from the conditions for the stability of a Fermi sphere with thermal diffuseness against small deformations.

Model calculations of the temperature dependence of the magnetization in the ordered phase and $T_c^{(1)}$ were performed earlier by Akhiezer *et al.*[4] These calculations did not take into account, e.g., the dependence of the Fermi-liquid function on the magnetic moment, of the form $\varphi(\sigma+\sigma')\mathbf{M}$, which gives a contribution to the free energy of the same order as that in Ref. 4.

In liquid $^3$He the quantity $1+Z_0 \approx 0.3$. Crude estimates from the available experimental data show that $\partial^2 Z_0/\partial\mu^2 > 0$, i.e., $\alpha_0 < 0$, and the paramagnetic state of $^3$He is evidently stable in the entire region of existence of the liquid phase.

The author is grateful to A. F. Andreev, I. E. Dzyaloshinskiĭ, M. I. Kaganov, and L. P. Pitaevskiĭ for very useful discussions and consultations.

[1]I. Ya. Pomeranchuk, Zh. Eksp. Teor. Fiz. **35**, 524 (1958) [Sov. Phys. JETP **8**, 361 (1959)].
[2]G. M. Éliashberg, Zh. Eksp. Teor. Fiz. **41**, 1241 (1961); **42**, 1658 (1962)[Sov. Phys. JETP **14**, 886 (1962); **15**, 1151 (1962)].
[3]L. D. Landau, Zh. Eksp. Teor. Fiz. **30**, 1058 (1956); **32**, 59 (1957); **35**, 97 (1958) [Sov. Phys. JETP **3**, 920 (1956); **5**, 101 (1957); **8**, 70 (1959)].
[4]I. A. Akhiezer, I. T. Akhiezer, and E. M. Chudnovskiĭ, Fiz. Nizk. Temp. **2**, 1321 (1976) [Sov. J. Low Temp. Phys. **2**, 645 (1976)].

Translated by P. J. Shepherd

# Natural optical activity in semiconductors with wurtzite structure

E. L. Ivchenko and A. V. Sel'kin

*A. F. Ioffe Physicotechnical Institute, USSR Academy of Sciences*
(Submitted 12 January 1979)
Zh. Eksp. Teor. Fiz. **76**, 1836–1855 (May 1979)

A theory is constructed of natural optical activity of crystals with wurtzite structure in the exciton-resonance frequency region. The reflection spectra are calculated for parallel and crossed polarizations of the incident and reflected light. The method of calculating the reflection coefficient is generalized to include the case of oblique incidence of the light for a generate exciton level, with allowance for dipole-forbidden states. Analysis of the limiting transition to the nonresonant region has made it possible to compare the conclusions of the developed microscopic theory with the results of the phenomenological approach. The reflection spectra of CdS at oblique incidence of light on the crystal boundary, in the region of the exciton resonance $B_{n=1}$ are experimentally investigated for the first time ever. The theoretical and experimental results are compared.

PACS numbers: 78.20.Ek, 78.20.Dj

## INTRODUCTION

Natural optical activity (NOA) can be possessed by crystals whose symmetry admits of linear terms in the expansion of the dielectric tensor $\varepsilon_{ij}(\omega, \mathbf{k})$ in powers of the wave vector $\mathbf{k}$.[1,2] The best known consequence of NOA is the rotation of the plane of polarization of a linearly polarized light wave when it propagates in an optically active medium. At the same time, there exist crystal classes $C_{3v}$, $C_{4v}$ and $C_{6v}$, which admit of NOA but do not have a rotating ability for any of the light-propagation directions.[3] In such crystals, just as in uniaxial inactive crystals, ordinary (transverse) and extraordinary (mixed) waves can be excited. However, as a result of the NOA the extraordinary waves in these crystals are elliptically polarized. The polarization ellipse lies in this case in the plane containing the hexagonal axis $C_6$ and the wave vector $\mathbf{k}$. The feasibility in principle of the existence of such waves and their experimental manifestations was apparently first pointed out in Refs. 3 and 4. Recently experimental observation of NOA was reported in the crystals CdS (Ref. 5) and AgI (Ref. 6) (crystal class $C_{6v}$).

The present paper is devoted to a theoretical and experimental investigation of NOA in the region of exciton resonance of crystals of the wurtzite type (symmetry $C_{6v}$). In the first part of the article we derive a system of material equations and obtain the energy spectrum of optical excitons in the region of exciton states $B_{n=1}$ with account taken of the terms linear in k in the exciton Hamiltonian (Secs. 1 and 2), we analyze the supplementary boundary conditions for a degenerate excitonic level, which are applicable for oblique incidence of light (Sec. 3) establish, by a limiting transition to the nonresonant region, the connection between the microscopic and phenomenological theories of NOA (Sec. 4), and present the results of a theoretical calculations of the reflection spectra with account taken of the NOA of crystals with wurtzite structure (Sec. 5). In the second part we describe the experimental procedure (Sec. 1), the results of the experimental investigation of the NOA in CdS crystals (Sec. 2), discuss the role of each of the parameters of the theory in the formation of the reflection

 0038-5646/79/050933-10$02.40  

spectra, and present a comparison of the experimental and theoretical results (Sec. 3).

## I. THEORY

### 1. The Material Equations

In $A_2B_6$ crystals with wurtzite structures (e.g., CdS and CdSe), depending on the symmetry of the excitonic state, a distinction is made between the excitons $A(\Gamma_7 \times \Gamma_9)$ and $B$ or $C(\Gamma_7 \times \Gamma_7)$. We consider NOA in the resonant frequency region corresponding to the exciton $B_n = 1$, since the effects of the NOA for excitons $B$ and $C$ should manifest themselves more strongly than those for excitons $A$ (see Sec. 2).

The ground state of exciton $B$ is split by the exchange interaction into a doubly degenerate level $\Gamma_5$ and two nondegenerate levels $\Gamma_1$ and $\Gamma_2$. In operations from group $C_{6v}$, the corresponding wave functions of the exciton are transformed like the components $(x, y)$, $z$ and $J_z$ ($J_z$ is the projection of an arbitrary pseudovector on the $C_6$ axis).

We confine ourselves henceforth to excitons with energy $\mathscr{E}_\nu(\mathbf{k})$ satisfying the inequality

$$|\mathscr{E}_\nu(\mathbf{k}) - \mathscr{E}_{\nu'}(0)| \ll |\Delta\mathscr{E}|, \tag{1}$$

where the indices $\nu$ and $\nu'$ number the states $\Gamma_{5x}$, $\Gamma_{5y}$, $\Gamma_1$, and $\Gamma_2$,

$$\mathscr{E}_\nu(\mathbf{k}) = \mathscr{E}_\nu(0) + \hbar^2 k_\perp^2/2M_\perp + \hbar^2 k_z^2/2M_\parallel, \tag{2}$$

$M_\perp$ and $M_\parallel$ are the translational masses of the exciton for the propagation directions $\mathbf{k} \perp \mathbf{c}$ and $\mathbf{k} \parallel \mathbf{c}$ ($\mathbf{c}$ is a unit vector in the direction of the $C_6$ axis), and $\Delta\mathscr{E}$ is the energy difference between the considered excitonic states and any other states.

We represent the wave function of the exciton in the form

$$\Psi^{(ex)}(\mathbf{r}, t) = \sum_\nu C_\nu(\mathbf{r}, t)\varphi_\nu, \tag{3}$$

where $\varphi_\nu$ is the wave function of the exciton at rest, $\mathbf{r}$ is the position of its center of gravity. Taking the Fourier transform in the temporal Schrödinger equation, we obtain, if the inequalities (1) are satisfied, a system of equations for the Fourier components $C_\nu(\mathbf{k}, \omega)$:

$$[\mathscr{E}_\nu(\mathbf{k}) - \hbar\omega]C_\nu(\mathbf{k}, \omega) + \sum_{\nu'} H_{\nu\nu'}(\mathbf{k})C_{\nu'}(\mathbf{k}, \omega) = \mathbf{d}_\nu(\mathbf{k})\mathbf{E}(\mathbf{k}, \omega), \tag{4}$$

where $\mathbf{E}(\mathbf{k}, \omega)$ is the amplitude of the electric field intensity, $\mathbf{d}_\nu(\mathbf{k}) = \langle\nu|\hat{\mathbf{d}}(\mathbf{k})|0\rangle$ is the matrix element of the dipole-moment density operator, corresponding to excitation of an exciton in a state $\nu$. The matrix $H_{\nu\nu'}(\mathbf{k})$ in (4) takes into account the terms linear in $\mathbf{k}$ in the energy spectrum of the excitons.[7-9] In the bases $\Gamma_{5x}$, $\Gamma_{5y}$, $\Gamma_1$, $\Gamma_2$, indicated above, this matrix takes the form[9]

$$\|H_{\nu\nu'}(\mathbf{k})\| = \begin{bmatrix} 0 & D \\ D^+ & 0 \end{bmatrix}, \quad D = i\begin{bmatrix} \beta_1 k_x, & -\beta_2 k_y \\ \beta_1 k_y, & \beta_2 k_x \end{bmatrix}, \tag{5}$$

where $\beta_{1,2}$ are real constants.

The components of the vector $\mathbf{d}_\nu(\mathbf{k})$, including corrections linear in $\mathbf{k}$, are listed in the table. There are altogether five independent constants ($\gamma_\parallel$, $\gamma_\perp$, $\alpha_\parallel$, $\alpha_\perp$, $\beta_\perp$), which determine these corrections. The real constants $d_\perp$ and $d_\parallel$ determine the matrix elements of the dipole-active transitions.

TABLE I. The matrix elements $d_{\nu i}(\mathbf{k})$ $(i = x, y, z)$ in the approximation linear in $\mathbf{k}$.

| $i$ | $\nu$ | | | |
|---|---|---|---|---|
| | $\Gamma_{5x}$ | $\Gamma_{5y}$ | $\Gamma_1$ | $\Gamma_2$ |
| $x$ | $d_\perp(1+i\gamma_\perp k_z)$ | 0 | $id_\parallel\alpha_\perp k_x$ | $id_\perp\beta_\perp k_y$ |
| $y$ | 0 | $d_\perp(1+i\gamma_\perp k_z)$ | $id_\parallel\alpha_\perp k_y$ | $-id_\perp\beta_\perp k_x$ |
| $z$ | $id_\perp\gamma_\parallel k_x$ | $id_\perp\gamma_\parallel k_y$ | $d_\parallel(1+i\alpha_\parallel k_z)$ | 0 |

The exciton contribution $\mathbf{P}(\mathbf{k}, \omega)$ to the polarization of the medium is connected with the coefficients $C_\nu(\mathbf{k}, \omega)$ by the relation

$$\mathbf{P}(\mathbf{k}, \omega) = \sum_\nu C_\nu(\mathbf{k}, \omega)\mathbf{d}_\nu^*(\mathbf{k}). \tag{6}$$

Taking the inverse Fourier transform $C_\nu(\mathbf{k}, \omega) \to C_\nu(\mathbf{r}, \omega)$ in (4) and introducing the notation

$$\begin{aligned} P_{0x} &= d_\perp C_{\Gamma_{5x}}(\mathbf{r}, \omega), \quad P_{0y} = d_\perp C_{\Gamma_{5y}}(\mathbf{r}, \omega), \\ P_{0z} &= d_\parallel C_{\Gamma_1}(\mathbf{r}, \omega), \quad Q = d_\perp C_{\Gamma_2}(\mathbf{r}, \omega), \end{aligned} \tag{7}$$

we can reduce the system (4) to the form

$$\begin{aligned} &[\mathscr{E}_{\Gamma_5}(-i\nabla) - \hbar\omega]\mathbf{P}_{0\perp} + \beta_1 \frac{d_\perp}{d_\parallel}\nabla_\perp P_{0z} \\ &+ \beta_2[\mathbf{c}\times\nabla Q] = d_\perp^2\left[\left(1+\gamma_\perp\frac{\partial}{\partial z}\right)\mathbf{E}_\perp + \gamma_\parallel\nabla_\perp E_z\right], \end{aligned} \tag{8}$$

$$\begin{aligned} &[\mathscr{E}_{\Gamma_1}(-i\nabla) - \hbar\omega]P_{0z} - \beta_1\frac{d_\parallel}{d_\perp}div\,\mathbf{P}_{0\perp} \\ &= d_\parallel^2\left[\alpha_\perp \operatorname{div}\mathbf{E}_\perp + \left(1+\alpha_\parallel\frac{\partial}{\partial z}\right)E_z\right], \end{aligned} \tag{9}$$

$$[\mathscr{E}_{\Gamma_2}(-i\nabla) - \hbar\omega]Q - \beta_2 \operatorname{rot}_z \mathbf{P}_{0\perp} = -d_\perp^2\beta_\perp \operatorname{rot}_z \mathbf{E}_\perp. \tag{10}$$

The contribution of the excitons to the polarization of the medium is expressed, according to (6) and the table, in terms of the quantities introduced in (7):

$$\begin{aligned} \mathbf{P}(\mathbf{r}, \omega) = &\left(1-\gamma_\perp\frac{\partial}{\partial z}\right)\mathbf{P}_{0\perp} + \left[\left(1-\alpha_\parallel\frac{\partial}{\partial z}\right)P_{0z}\right. \\ &\left. - \gamma_\parallel \operatorname{div}\mathbf{P}_{0\perp}\right]\mathbf{c} - \alpha_\perp\nabla_\perp P_{0z} + \beta_\perp[\mathbf{c}\times\nabla Q]. \end{aligned} \tag{11}$$

Consequently, in the zeroth approximation in $\mathbf{k}$ for the matrix elements in $\mathbf{d}_\nu$, the vector $\mathbf{P}_0 = (P_{0x}, P_{0y}, P_{0z})$ coincides with the excitonic contribution to the polarization. We note that Eqs. (8)–(10) for $\mathbf{P}_0$ and $Q$ could be obtained in general form from symmetry considerations alone. However, the derivation presented here is made it possible to establish the connection between some of the coefficients in these equations.

Expression (11) and Eqs. (8)–(10) constitute the system of material equations which together with Maxwell's equations form a closed system.

### 2. Energy Spectrum of the Optical Excitons

The influence of terms linear in $\mathbf{k}$ on the energy spectrum of the Coulomb excitons was analyzed in detail in Ref. 9. In the present section we obtain the spectrum of the optical excitons (polaritons), i.e., we take the retardation into account. The dispersion relations for the polaritons are obtained from the condition for the existence of nonzero solutions of the simultaneous system of

equations (8)–(11) and Maxwell's equations. Another method, which of course leads to the same results is based on the solution of the equation

$$(ck/\omega)^2\mathbf{E}_{tr}=\hat{\varepsilon}_0\mathbf{E}+4\pi\hat{\beta}\mathbf{E}_{tr}, \tag{12}$$

where $\mathbf{E}_{tr}$ is the transverse component of the vector $\mathbf{E}$ (relative to the vector $\mathbf{k}$), $\hat{\varepsilon}_0$ is the tensor of the background dielectric constant, and $\hat{\beta}$ is the contribution of the Coulomb excitons $B$ to the polarizability tensor. The expression for $\hat{\beta}(\omega, \mathbf{k})$ can be obtained by using the energy spectrum and the selection rules for the Coulomb excitons, which were calculated in Ref. 9.

For simplicity we consider henceforth the case $\mathbf{k}\perp\mathbf{c}$, which corresponds to the geometry of the experiments of Refs. 5 and 6, and neglect the linear corrections to the matrix elements $\mathbf{d}_\nu(\mathbf{k})$.

The indicated closed system of equations has two types of solutions: transverse modes and mixed modes. For the transverse modes ($\mathbf{E}\perp\mathbf{k}$ and $\mathbf{E}\perp\mathbf{c}$), in the case $\mathbf{k}\perp\mathbf{c}$ the dispersion equation takes the form

$$\left[\mathscr{E}_{\Gamma_5}(\mathbf{k})-\hbar\omega-\frac{\hbar\omega_{LT}{}^{\perp}\varepsilon_{0\perp}}{(ck/\omega)^2-\varepsilon_{0\perp}}\right](\mathscr{E}_{\Gamma_5}(\mathbf{k})-\hbar\omega)=\beta_2{}^2k^2. \tag{13}$$

In the case of mixed modes, the vector $\mathbf{E}$ lies in the ($\mathbf{k}$, $\mathbf{c}$) plane, and the dispersion equation for them takes the form

$$\left[\mathscr{E}_{\Gamma_1}(\mathbf{k})-\hbar\omega-\frac{\hbar\omega_{LT}{}^{\parallel}\varepsilon_{0\parallel}}{(ck/\omega)^2-\varepsilon_{0\parallel}}\right](\mathscr{E}_{\Gamma_1}(\mathbf{k})-\hbar\omega+\hbar\omega_{LT}{}^{\perp})=\beta_1{}^2k^2. \tag{14}$$

In (13) and (14) we have introduced the following notation: $\varepsilon_{0\perp}$, $\varepsilon_{0\parallel}$ is the background dielectric constant for the polarization $\mathbf{E}\perp\mathbf{c}$ and $\mathbf{E}\parallel\mathbf{c}$; $\hbar\omega_{LT}{}^{\perp}=4\pi d_\perp^2/\varepsilon_{0\perp}$ and $\hbar\omega_{LT}{}^{\parallel}=4\pi d_\parallel^2/\varepsilon_{0\parallel}$ are the longitudinal-transverse splittings for the states $\Gamma_5$ and $\Gamma_1$.

Each of the dispersion equations (13) and (14) is cubic in $k^2$, meaning the existence of three transverse and three mixed modes. Therefore the total number of modes is equal to six in accordance with the two states of polarization of the external photon and the fourfold degeneracy of the exciton $B$ in the ground state. Since all the coefficients in (13) and (14) are real, the roots of each of them are either all real or else one of them is real and the two others are complex conjugate. The real negative and complex roots correspond to damped modes.

According to (13) and (14), the constant $\beta_1$ in the case of terms linear in $\mathbf{k}$ leads to a mixing of the polaritons $\Gamma_1$ with longitudinal excitons $\Gamma_5$, while the constant $\beta_2$ leads to a mixing of the polaritons $\Gamma_5$ with the dipole-forbidden excitons $\Gamma_2$.

Figure 1 shows the characteristic energy spectra of the polaritons $B_{n=1}$ for two cases: $\beta_1=\beta_2=0$ (Figs. 1a and b) and $\beta_2\omega_0/c=0.05$ meV, $\beta_1=-\beta_2$ (Ref. 9) (Figs. 1c and 1d), where $\omega_0=\mathscr{E}_0/\hbar$ is the resonant frequency of the exciton $B$. In the calculation we used the following values of the parameters: $\mathscr{E}_0=\hbar\omega_0=2.568$ eV, $\hbar\omega_{LT}^{\perp}=1.4$ meV, $\hbar\omega_{LT}^{\parallel}=2.1$ meV, $M_\perp=1.3m_0$, $\varepsilon_{0\perp}=8.3$, $\varepsilon_{0\parallel}=8.6$ ($m_0$ is the mass of the free electron), and neglected the exchange splitting of the exciton $B$. The solid curves in Fig. 1 correspond to real parts of $k$, and the dashed ones to the imaginary parts. Figures 1a and 1c show the

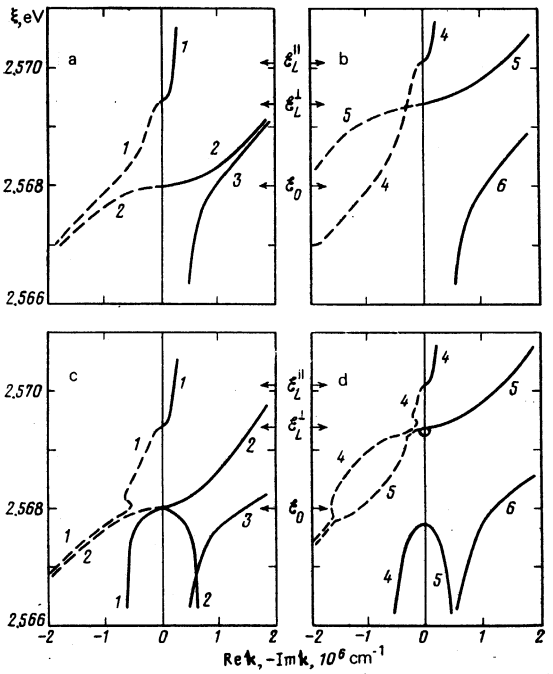


FIG. 1. Energy spectrum of optical excitons without (a, b) and with (c, d) allowance for the terms linear in $\mathbf{k}$ in the exciton Hamiltonian: 1, 2, 3—transverse modes (a, c), 4, 5, 6—mixed modes (b, d). The solid curves are plots of the energy of the optical excitons against the real part of $\mathbf{k}$, and the dashed are plots of the imaginary parts. The numerical values of the parameters used in the calculation are given in the text.

dispersion curves of the transverse modes 1, 2, and 3, while Figs. 1b and 1d show the dispersion branches of the mixed modes 4, 5, and 6. A comparison of Figs. 1a, c with Figs. 1b, d demonstrates clearly the influence of the terms linear in $k$ on the energy spectra of the excitons.

Solution of the system of Eqs. (8)–(10) makes it possible to find the exciton contribution to the polarizability of the crystal and consequently also to the dielectric tensor $\varepsilon_{ij}(\omega, \mathbf{k})$. In particular, the contribution of the exciton to the off-diagonal components $\varepsilon_{xz}=-\varepsilon_{zx}$ and $\varepsilon_{yz}=-\varepsilon_{zy}$ is

$$\begin{aligned}\varepsilon_{zx}&=i\gamma(\omega,\mathbf{k})k_x,\ \varepsilon_{yz}\\&=i\gamma(\omega,\mathbf{k})k_y;\\ \gamma(\omega,\mathbf{k})&=-\frac{\hbar\beta_1(\varepsilon_{0\perp}\varepsilon_{0\parallel}\omega_{LT}{}^{\perp}\omega_{LT}{}^{\parallel})^{1/2}}{[\mathscr{E}(\mathbf{k})-\hbar\omega]^2}.\end{aligned} \tag{15}$$

The ellipticity of the mixed modes is determined by the parameter $\beta_1$. At the same time, the constant $\beta_2$ does not change the state of polarization of the polaritons, since it does not lead to expressions for $\varepsilon_{xz}$ and $\varepsilon_{yz}$. Consequently the NOA in the vicinity of the exciton resonance is connected with the constant $\beta_1$. It can be shown that the terms linear in $\mathbf{k}$ in the energy spectrum of the exciton $A$ ($\Gamma_7\times\Gamma_9$) do not lead to NOA. This explains, in particular, our choice of exciton $B$ for the analysis.

## 3. Boundary Conditions

To observe NOA experimentally in CdS and AgI crys-

tals, the reflection spectra were investigated[5,6] in polarized light obliquely incident on the crystal boundary. In accordance with the experimental geometry of the cited papers, we consider henceforth the case when the $C_6$ axis is perpendicular to the plane of incidence and lines in the plane of the reflecting face of the crystal (Fig. 2).

In the general case the connection between the $p$ and $s$ components of the indicent and reflected light can be represented in the form

$$\begin{pmatrix} E_p \\ E_s \end{pmatrix} = \begin{pmatrix} r_{pp} & r_{ps} \\ r_{sp} & r_{ss} \end{pmatrix} \begin{pmatrix} E_{0p} \\ E_{0s} \end{pmatrix}, \tag{16}$$

where $\mathbf{E}_0$ and $\mathbf{E}$ are the amplitudes of the incident and reflected waves, the index $s$ ($p$) corresponds to the component of the vector $\mathbf{E}_0$ or $\mathbf{E}$ parallel (perpendicular) to the $C_6$ axis. The reflection coefficeints $r_{pp}$, $r_{ss}$, $r_{ps}$ and $r_{sp}$ depend on the frequency $\omega$ and on the incidence angle $\varphi$. By virtue of the invariance of the system to time reversal and by virtue of the symmetry of the considered reflection geometry (see Fig. 2), the off-diagonal coefficients $r_{ps}$ and $r_{sp}$ should coincide.

In the calculation of the reflection coefficients in the exciton region of the spectrum it is necessary, as is well-known to specify supplementary boundary conditions (SBC).[1,10] In the considered case of the exciton $B_{n=1}$, there should be four such conditions. We use SBC in the form

$$\mathbf{P}_0|_{y=0}=0, \quad Q|_{y=0}=0. \tag{17}$$

At normal incidence of light, and without taking into account the terms linear in $\mathbf{k}$, the SBC (17) go over into the frequently used SBC that correspond to the vanishing of the exciton polarization on the boundary. At $\beta_1=\beta_2=0$ and $d_\parallel=0$, the SBC (17) reduce to the condition $\mathbf{P}_{0\perp}|_{y=0}=0$, which was used previously to calculate the reflection coefficient in the region of the exciton $A$ in the crystals CdS and CdSe.[11,12] Finally, the conditions (17) constitute a generalization, to the case of oblique incidence of the light, of the SBC used by Mahan and Hopfield[8] to calculate the reflection spectrum in normal incidence with account taken of the terms linear in $\mathbf{k}$.[8]

The conditions (17) can be obtained by following the derivation of the SBC in Refs. 10, 13, and 14, if the length of the polariton wave exceeds the radius of the exciton and if the wave functions of the mechanical excitons vanish on the crystal boundary. To take into account the singularities of the behavior of the wave function of the exciton near the boundary, we can make use of the concept of the excitonless transition or "dead" layer[15] and specify the SBC (17) on the inner surface of this layer.

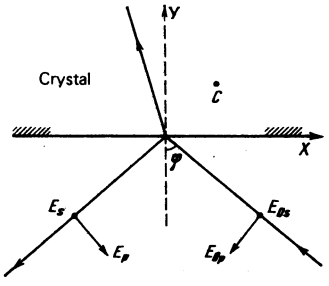


FIG. 2. Geometry of the reflection. Positive directions of the $p$-components of the incident and reflected light are marked by arrows, and the positive direction of the $s$ components coincides with the direction of the $z$ axis ($C_6$ axis) of the coordinate system.

The SBC (17) can be transformed to the following form, which is convenient for calculations:

$$\sum_{l=1}^{3}(n_l^2-\varepsilon_{0\perp})E_i^{(l)}-\varepsilon_{0\perp}\sum_{l'=4}^{6}E_i^{(l')}=0 \quad (i=x,y), \tag{18}$$

$$\sum_{l=4}^{6}(n_l^2-\varepsilon_{0\parallel})E_z^{(l)}=0, \tag{19}$$

$$\sum_{l=1}^{3}\frac{1}{n_l^2}\{[\mathscr{E}_{\Gamma_5}(\mathbf{k}_l)-\hbar\omega](n_l^2-\varepsilon_{0\perp})-\hbar\omega_{LT}^{\perp}\varepsilon_{0\perp}\}[\mathbf{n}_l\times\mathbf{E}^{(l)}]_z=0, \tag{20}$$

where the index $l$ numbers the transverse (1, 2, 3) and mixed (4, 5, 6) modes; $\mathbf{n}_l=c\mathbf{k}_l/\omega$ is the refraction vector, and $\mathbf{E}^{(l)}$ is the amplitude of the electric field intensity of the $l$-th mode excited inside the crystal when a plane monochromatic light wave is incident on the boundary.

The Maxwell boundary conditions, i.e., the conditions of continuity of the tangential components of the vectors $\mathbf{E}$ and $\mathbf{B}$, take in our case the form

$$\begin{aligned} &E_{0s}+E_s=\sum_{l=4}^{6}E_z^{(l)}, \quad (E_p-E_{0p})\cos\varphi=\sum_{l=1}^{3}E_x^{(l)}, \\ &E_p+E_{0p}=\sum_{l=1}^{3}n_lE^{(l)}, \quad (E_{0s}-E_s)\cos\varphi=\sum_{l=4}^{6}n_{l,y}E_z^{(l)}. \end{aligned} \tag{21}$$

The transverse modes satisfy the relations

$$E_z^{(l)}=0, \quad E_x^{(l)}=-\frac{n_{l,y}}{n_l}E^{(l)}, \quad E_y^{(l)}=\frac{n_{l,x}}{n_l}E^{(l)}. \tag{22}$$

For the mixed modes we have

$$\begin{aligned} &\mathbf{E}_\perp^{(l)}=\frac{\mathbf{n}_l}{n_l}E_\perp^{(l)}, \quad E_\perp^{(l)}=\Phi_lE_z^{(l)}, \\ &\Phi_l=-i\beta_1k_0\left(\frac{\omega_{LT}^{\perp}\varepsilon_{0\perp}}{\omega_{LT}^{\parallel}\varepsilon_{0\parallel}}\right)^{1/2}\frac{n_l(n_l^2-\varepsilon_{0\parallel})}{\varepsilon_{0\perp}[\mathscr{E}(\mathbf{k})-\hbar\omega+\hbar\omega_{LT}^{\perp}]}. \end{aligned} \tag{23}$$

The Maxwell boundary conditions (21) together with the SBC (17) agree with the energy conservation law. In fact, following Ref. 16, the pointing relation can be rewritten in the form of an energy conservation law with an energy flux density vector

$$\begin{aligned} \mathbf{S}(\mathbf{r},t)=&\frac{c}{4\pi}[\mathbf{E}\times\mathbf{B}]-\frac{\beta_1}{d_\perp d_\parallel}\dot{P}_{0z}\mathbf{P}_{0\perp} \\ &+\frac{\beta^2}{d_\perp^2}[\dot{\mathbf{P}}_{0\perp}\times\mathbf{c}]Q-\sum_{i=x,y}\frac{\hbar^2}{d_\perp^2}\dot{P}_{0i}\hat{\mu}\nabla P_{0i} \\ &-\frac{\hbar^2}{d_\parallel^2}\dot{P}_{0z}\hat{\mu}\nabla P_{0z}-\frac{\hbar^2}{d_\perp^2}Q\hat{\mu}\nabla Q-\gamma_\perp(\dot{\mathbf{P}}_{0\perp}\mathbf{E}_\perp)\mathbf{c} \\ &-\gamma_\parallel E_z\dot{\mathbf{P}}_{0\perp}-\alpha_\perp\dot{P}_{0z}\mathbf{E}_\perp+\alpha_\parallel\dot{P}_{0z}E_z\mathbf{c}+\beta_\perp[\mathbf{E}_\perp\times\mathbf{c}]Q, \end{aligned} \tag{24}$$

where $(\hat{\mu}\nabla)_i=(1/2M_{ii})\nabla_i$, $M_{zz}=M_\parallel$, $M_{xx}=M_{yy}=M_\perp$. For the sake of generality, Eq. (24) takes into account all the corrections listed in the table. We note the Exp. (24) for the energy flux density was determined uniquely, accurate to terms that can be transformed into a total derivative with respect to time or to a curl of a certain vector. It can be verified that the boundary conditions

(17) and (21) ensure continuity of the normal components of the energy flux density (24) through the crystal boundary.

## 4. Limiting Transition to the Long-Wave Region of the Spectrum

In the present section we analyze the limiting case when

$$\frac{|\beta_1|k_0}{\mathscr{E}_\nu(0)-\hbar\omega}\ll 1, \quad \frac{\delta\mathscr{E}}{\mathscr{E}_\nu(0)-\hbar\omega}\ll 1, \tag{25}$$

where

$$\delta\mathscr{E}=\max\left\{|\beta_2|k_0, \frac{\hbar^2\varepsilon_{0\perp}}{2M_\perp}k_0^2, \hbar\omega_{LT}^{\perp\parallel}, |\mathscr{E}_\nu(0)-\mathscr{E}_{\nu'}(0)|\right\}, \quad k_0=\omega/c.$$

As before, we assume the following inequalities to be satisfied

$$\hbar\omega\gg\mathscr{E}_\nu(0)-\hbar\omega, \tag{26}$$

in order that the condition (1) be satisfied and that the system (8)–(10) be valid. In the frequency region specified by the inequalities (25) and (26), the system (18)–(21) can be solved without a computer. It then becomes possible to compare the conclusions of the microscopic NOA theory developed in the present paper with the results of a phenomenological analysis of the reflection spectra in gyrotropic crystals.[14,17]

According to (15), the dielectric tensor $\varepsilon_{ij}(\omega, \mathbf{k})$ takes in the approximation linear in $\mathbf{k}$ the form

$$\|\varepsilon_{ij}(\omega, \mathbf{k})\|=\begin{bmatrix}\varepsilon_\perp & 0 & i\gamma k_x\\ 0 & \varepsilon_\perp & i\gamma k_y\\ -i\gamma k_x & -i\gamma k_y & \varepsilon_\parallel\end{bmatrix}, \tag{27}$$

where

$$\gamma(\omega)=-\beta_1\frac{(\varepsilon_{0\perp}\varepsilon_{0\parallel}\omega_{LT}^{\perp}\omega_{LT}^{\parallel})^{1/2}}{\hbar(\omega_0-\omega)^2}, \tag{28}$$

$\omega_0$ is the resonant frequency of the mechanical exciton at $\mathbf{k}=0$ without allowance for the exchange interaction. The terms linear in $\mathbf{k}$ in the expression for the tensor $\varepsilon_{ij}(\omega, \mathbf{k})$ determine the NOA of the crystals in the frequency region specified by the inequalities (25) and (26). The macroscopic parameter $\gamma(\omega)$ and the constant $\beta_1$ are then connected by the simple relation (28).

In our case, when the plane of incidence is perpendicular to the $C_6$ axis, the coefficients $r_{sp}$ and $r_{ps}$ differ from zero only when the NOA is taken into account. Namely, observation of the reflection in crossed polarizations ($s\to p$ or $p\to s$ at an incidence angle $\varphi\neq 0°$) was in fact used in Ref. 5 to observe NOA in CdS crystals. In the frequency regions (25) and (26) we therefore calculate the reflection coefficients in first order in $|\gamma|k_0 \ll 1$, and neglect corrections of the order

$$[\beta_1 k_0/\hbar(\omega_0-\omega)]^2, \quad [\delta\mathscr{E}/\hbar(\omega_0-\omega)]^2,$$

which make no contribution to $r_{ps}$ and $r_{sp}$. In the indicate approximation, we can neglect the excitation of the excitonic state $\Gamma_2$, assuming in (13) that $\beta_2=0$ and disregarding Eq. (20) in the solution of the system of equations (18)–(21). In Eqs. (18) and (21) we must put $\mathbf{E}^{(3)}=0$, i.e., we assume that in the crystal are excited not three but two transverse waves. One is a volume wave ($l=1$) with a refractive index

$$n_1=\varepsilon_{0\perp}^{1/2}\left(1+\frac{1}{2}\frac{\omega_{LT}^{\perp}}{\omega_0-\omega}\right), \tag{29}$$

and the other ($l=2$) is the surface wave and attenuates in the interior of the crystal like $\exp(-\alpha_2 y)$, where

$$\alpha_2\approx[2M_\perp(\omega_0-\omega)/\hbar]^{1/2},$$

with $\alpha_2\gg k_0 n_\perp$.

The solutions of the dispersion equation (14) for mixed waves can be represented in the considered frequency region in the form

$$n_4=\varepsilon_{0\parallel}^{1/2}\left(1+\frac{1}{2}\frac{\omega_{LT}^{\parallel}}{\omega_0-\omega}\right),$$

$$n_{5,6}^2=-\frac{2M_\perp}{\hbar k_0^2}\left\{\omega_0-\omega+\frac{1}{2}\left(\omega_{LT}^{\perp}-\frac{2M_\perp\beta_1^2}{\hbar^3}\right)\right. \tag{30}$$

$$\left.\pm\left[\frac{1}{4}\left(\omega_{LT}^{\perp}-\frac{2M_\perp\beta_1^2}{\hbar^3}\right)^2-\frac{2M_\perp\beta_1^2}{\hbar^3}(\omega_0-\omega)\right]^{1/2}\right\},$$

with $|n_{5,6}^2|\gg 1$.

At $M_\perp\beta_1^2/\hbar^3>2(\omega_0-\omega)$ the quantities $n_5$ and $n_6$ are real, and the states 5 and 6 correspond to short-wave volume excitation; at $M_\perp\beta_1^2/\hbar^3<2(\omega_0-\omega)$ the waves 5 and 6 attenuate in the interior of the crystal.

We express the amplitudes of the waves 2, 5, and 6 in terms of the amplitudes of the volume waves 1 and 4, using the SBC in the form (18) and (19), and substitute the obtained expressions in the Maxwell boundary conditions (21). As a result we obtained in first-order approximation in $|\gamma|k_0\ll 1$, the following system of equations for the amplitudes $\mathbf{E}_0$, $\mathbf{E}$, $\mathbf{E}^{(1)}$ and $\mathbf{E}^{(4)}$:

$$\begin{aligned}\mathbf{E}_\tau(-0)&=\mathbf{E}_\tau(+0)+\tilde{\mathbf{E}}(+0),\\ \mathbf{B}_\tau(-0)&=\mathbf{B}_\tau(+0)+\tilde{\mathbf{B}}(+0),\end{aligned} \tag{31}$$

where the magnetic-field induction vector is $\mathbf{B}=-ik_0^{-1}\,\mathrm{curl}\,\mathbf{E}$; $\mathbf{E}_\tau$ and $\mathbf{B}_\tau$ are the tangential components of the vectors $\mathbf{E}$ and $\mathbf{B}$, $\mathbf{E}(\pm 0)$ are the values of the vector $\mathbf{E}$ on the boundary of the crystal at $y>0$ (medium) and $y<0$ (vacuum), $\mathbf{E}(+0)=\mathbf{E}^{(1)}+\mathbf{E}^{(4)}$; the contributions of the waves 5 and 6

$$E_z=0, \quad E_x=\frac{\gamma}{2\varepsilon_{0\perp}}\frac{\partial E_z}{\partial x}, \quad B_z=0, \quad B_x=\frac{\gamma}{2\varepsilon_{0\perp}}\frac{\partial B_z}{\partial x}, \tag{32}$$

do not depend on the effective mass of the exciton and there is no contribution from the wave 2 in this approximation. The form of the equation (31) does not depend on the relation between $M_\perp\beta_1^2/\hbar^3$ and $\omega_0-\omega$.

Solving (31), we found that in first-order approximation in $|\gamma|k_0\ll 1$ the expressions for the diagonal coefficients $r_{pp}$ and $r_{ss}$ coincide with the known Fresnel formulas obtained neglecting NOA, and the off-diagonal coefficients of

$$r_{sp}=r_{ps}=\frac{1}{2}\frac{i\gamma k_0\sin(2\varphi)}{((\varepsilon_{0\parallel}-\sin^2\varphi)^{1/2}+\cos\varphi)((\varepsilon_{0\perp}-\sin^2\varphi)^{1/2}+\varepsilon_{0\perp}\cos\varphi)}. \tag{33}$$

Calculation of the reflection coefficients in the nonresonant region for the crystals of symmetry $C_{3v}$, $C_{4v}$, $C_{6v}$ were made also in Ref. 4. The expression obtained there for $r_{sp}=r_{ps}$, contained, unlike (33), a factor 1/2. In the

calculation of Ref. 4, account was taken of only two waves excited in the crystal and corresponding to waves 1 and 4 considered above, but corrections were introduced in Maxwell's boundary conditions. The boundary conditions used in Ref. 4 can be represented in the form similar to (31) by putting $\tilde{\mathbf{E}}_\tau = 0$ in (31) and multiplying the vector $\tilde{\mathbf{B}}_\tau$, defined in accordance with (32), by two. We note in this connection that in this approximation the system (31), in which $\tilde{\mathbf{E}}_\tau$ is replaced by $t_1\tilde{\mathbf{E}}_\tau$ and $\tilde{\mathbf{B}}_\tau$ is replaced by $t_2\tilde{\mathbf{B}}_\tau$, agrees with the energy conservation law at arbitrary $t_1$ and $t_2$ satisfying the condition $t_1 + t_2 = 2$. We attribute the indicated difference between (33) and the results of Ref. 4 to the fact that in Ref. 4 no account was taken of the influence of the additional short-wave modes on the reflection coefficients.

The form of the additional terms in (31) depends on the symmetry of the crystal. We have analyzed also the case of gyrotropic crystals of cubic symmetry (point group $T$ or 0) in the frequency region specified by inequalities similar to (25) and (26):

$$|\beta|k_0, \hbar\omega_{LT}, \hbar^2\varepsilon_0 k_0^2/2M \ll \hbar(\omega_0 - \omega) \ll \hbar\omega,$$

where $\omega_0$ is the resonant frequency of the optically active exciton, and $\beta$ is a constant for the terms linear in $\mathbf{k}$ in the energy spectrum of the exciton. In this case there is no correction to the first equation of (31), and the expression for $\tilde{\mathbf{B}}_\tau$ coincides with the corrections to the Maxwell boundary conditions, which were introduced in Refs. 4 and 17.

### 5. Resonance Conditions

Far from the resonant absorption bands, the quantity $r_{ps}$ is of the order $a/\lambda \ll 1$, where $a$ is a characteristic microscopic dimension (of the order of the lattice constant) and $\lambda$ is the wavelength of the light in the crystal. In nonresonant conditions it is therefore difficult to register the NOA. However, in the resonance region of frequencies, when $\lambda$ is substantially decreased, the effects produced by the NOA should become considerably enhanced (as should any effect due to spatial dispersion[1]).

Figure 3 shows the spectral dependences of the energy coefficients of reflection $R_{pp} = |r_{pp}|^2$ (a) and $R_{ss} = |r_{ss}|^2$ (b) for the case of normal incidence (dashed curves), and also the spectral dependences of the "off-diagonal" coefficients $R_{sp} = |r_{sp}|^2$ (a) and $R_{ps} = |r_{ps}|^2$ (b) for the case of oblique incidence at an angle 45° (solid curves), calculated with a computer. In the calculations we used the parameters given above and SBC of the type (17), and took into account a surface transition layer $l = 70$ Å thick. In addition, we introduced exciton damping $\Gamma = 0.05$ meV, the same for all four states.

Attention is called to the clearly pronounced resonant character of the spectral dependences of the off-diagonal coefficients $R_{sp}$ and $R_{ps}$, which reach a maximum value at an energy $\mathscr{E}_L^\perp$ of the longitudinal exciton $\Gamma_5$. At $\beta_1 = 0$ there is no orthogonal component in the reflection spectrum ($R_{ps} = R_{sp} = 0$), and with increasing $\beta_1$ the maximum values of $R_{sp}$ and $R_{ps}$ increase. It can be shown that in analogy with (33) at normal incidence this effect is absent. The coefficients $R_{sp}$ and $R_{ps}$ coincide, as they should.

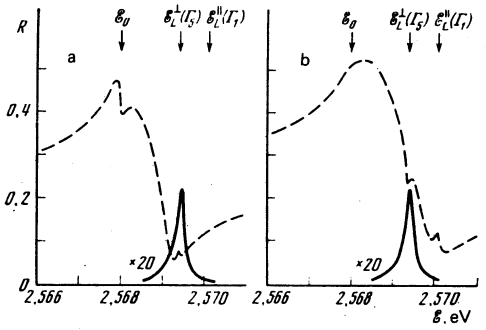


FIG. 3. Theoretical reflection spectra in the region of the exciton resonance $B_{n=1}$ in parallel (dashed curves) and crossed (solid) polarizations: $R_{pp}$ (a) and $R_{ss}$ (b) at $\varphi = 2°$, $R_{sp}$ (a) and $R_{ps}$ (b) at $\varphi = 45°$. The numerical parameters are the same as in Figs. 1c and 1d.

The experimental dependences of the reflection coefficients $R_{pp}$ and $R_{ss}$ (dashed curves in Fig. 3) also have a number of singularities. The $R_{pp}$ spectrum (Fig. 3a) is similar to the reflection spectra in the $p$ component, calculated in Ref. 8. The additional structure in the region of the principal maximum of the reflection near the resonant energy $\mathscr{E}(0)$ is due to the constant $\beta_2$. The small spike in the region of the principal minimum at the energy $\mathscr{E}_L^\perp$ of the longitudinal exciton $\Gamma_1$ is due to the transition layer. The spectrum of $R_{ss}$ (Fig. 3b) has singularities in the form of a local minimum on the short-wave slope of the reflection curve (energy $\mathscr{E}_L^\perp$) and in the form of a spike at the energy $\mathscr{E}_L^\parallel$ of the longitudinal exciton $\Gamma_1$ in the region of the principal minimum. The first singularity arises at $\beta_1 \neq 0$, i.e., it is due to the mixing of the states of the longitudinal and transverse excitons $\Gamma_5$ and $\Gamma_1$. The second singularity is due to the transition layer.

## II. EXPERIMENT

### 1. Experimental Procedure

We investigated in the experiment single-crystal plates of cadmium sulfide (≈4×3×0.1 mm), grown from the gas phase. The reflecting phase was a natural-growth plane parallel to the hexagonal axis of the crystal. The investigations were made on crystals whose reflection spectra in the spectral region of the excitons $A$ and $B$ $T \leq 4.2$ K, normal incidence) were similar to those given in Refs. 8 and 15. The latter served as a criterion for good quality of the crystals.

The crystals were immersed directly in liquid helium whose vapor was pumped up, making it possible, on the one hand, to lower the temperature to 2 K, and on the other hand to reduce to a minimum the noise due to the boiling of the helium. The reflections spectra were registered photoelectrically (using a photon-counting system) with a DFS-24 spectrometer. A depolarizing wedge was placed ahead of the entrance slit of the spectrometer to eliminate the undesirable influence of the optical polarization of the instrument.

The incidence angle $\varphi$ could be varied in the range from 5 to 85° and set with an accuracy ±1°. The light

source was an incandescent lamp. The crystal was placed between the polarizer and analyzer, whose azimuths could be varied and measured with the aid of angle-measuring devices.

The experimental setup made it possible to measure reliably the reflection spectra in relative units. To determine the absolute values it was sufficient to know the absolute value of the reflection coefficient at any one frequency. To this end we took into account the fact that according to the Fresnel formulas for anisotropic medium, at an incidence angle $\varphi = 45°$, regardless of the value of the dielectric constant, the following relation holds

$$R_{ss}(45°) = R_{pp}(45°)/R_{ss}(45°). \quad (34)$$

Thus, if we measure in relative units the coefficients $R_{pp}(45°)$ and $R_{ss}(45°)$ at one of the frequencies in a spectral region far from the exciton resonances, where the Fresnel formulas are valid, then formula (34) can be used to obtain also the absolute value of the coefficient $R_{ss}(45°)$ at this frequency. Using the obtained value of $R_{ss}(45°)$, it is possible to calculate with Fresnal formulas the dielectric constant and determine the coefficients $R_{pp}$ and $R_{ss}$ at arbitrary incidence angles.

In uniaxial crystals, owing to the optical anistropy, the relation (34) is not satisfied in the general case. However, in CdS crystals far from the resonant region of the spectrum, on the long-wave side, there exists a wavelength $\lambda_{is}$ ("isotropic point")[18] on which the refractive indices of the ordinary and extraordinary rays coincide, i.e., on which the crystal becomes optically isotropic and formula (34) is valid. The exact position of the "isotropic point" for the samples employed by us was determined by us from the spectral position of the minimum, closest to $\lambda_{is}$ (according to the data of Ref. 18), of the transmission of the crystal placed between the crossed polarizer and analyzer, (the polarization planes of the analyzer and the polarizer made in this case an angle of 45° with the optical axis of the crystal).

We checked on the position of the "isotropic point" by using crystals of different thicknesses, since the minimum of the interference pattern of the transmission, corresponding to $\lambda_{is}$, should have the same spectral position regardless of the crystal thickness. To eliminate the influence of the wave reflected from the rear face of the crystal (the "isotropic point" in CdS is located in the transparency region), the measurements were made on wedge-shaped samples.

Following the procedure described above, we determined the position of the "isotropic point" $\lambda_{is} = 5098$ Å (2.432 eV) and the corresponding value of the dielectric constant $\varepsilon_{is} = 7.67$ at $T = 2$ K. The solid curve in Fig. 4 shows the theoretical dependence of the ratio $R_{pp}/R_{ss}$ on the incidence angle $\varphi$, constructed for $\varepsilon_{is} = 7.67$. The experimental points obtained for the incidence angles 8, 30, and 45° agree well with this curve. At large incidence angles ($\varphi > 80°$) the angle-measurement error leads to a large error in the measurement of the reflection coefficients. In these cases the actual angle $\varphi$ was chosen by us to be the angle corresponding in accordance with the Fresnel formulas to the experimentally

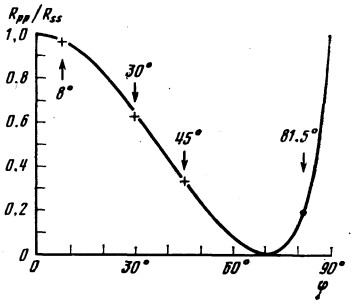


FIG. 4. Ratio $R_{pp}/R_{ss}$ of the reflection coefficients vs. the incidence angle $\varphi$ at the frequency of the "isotropic point" of the CdS crystal ($T = 2$ K). Solid curve—result of calculation. The encircled point on the curve corresponds to the experimentally determined ratio $R_{pp}/R_{ss}$, from which the angle $\varphi$ is determined at "glancing" incidence.

measured ratio $R_{pp}/R_{ss}$. In particular, the experimentally obtained ratio $R_{pp}/R_{ss} = 0.193$ should be satisfied at $\varphi = 81.5°$ (the dark point in Fig. 4).

The reflection spectra registered in the exciton region of the spectrum were normalized to the values of the reflection coefficients in the "isotropic point." The accuracy of the measurement of the absolute values of the reflection coefficient in this method is approximately 5%. The greatest accuracy is reached at an incidence angle $\varphi = 45°$, for which the normalization is carried out directly by formula (34).

## 2. Experimental Results

Figure 5 shows the experimentally measured reflection spectra of CdS crystal at $T = 2$ K for incidence angles equal to 8° (a, b) 45° (c, d), and 81.5° (e, f) in the region of the exciton resonance $B_{n=1}$. The geometry of the experiment is shown in Fig. 2. The light circles represent the values of the coefficients $R_{pp}$ (a, c, e) and $R_{ss}$ (b, d, f); the dark circles correspond to the reflection coefficients $R_{sp}$ (a, c, e) and $R_{ps}$ (b, d, f) in the orthogonal configurations.

At almost normal incidence ($\varphi = 8°$) the $R_{pp}$ and $R_{ss}$ reflection spectra are similar to the spectra discussed in Ref. 8. Just as in that reference, a distinct supplementary structure is observed in the region of the principal maximum of the $R_{pp}$ spectrum, while the $R_{ss}$ spectrum has no structure. There are no singularities whatever in the region of the principal minima. Attention is called to the fact that the minimum in the $R_{ss}$ spectrum is shifted somewhat in the short-wave side away from the principal minimum of the spectrum $R_{pp}$.

When the incidence angle is increased to 45°, the supplementary structure in the region of the principal maximum of the $R_{pp}$ spectrum is retained, and in the region of the principal minimum there appears a singularity in the form of a small spike (Fig. 5c). At the same time, the spectrum $R_{ss}$ retains its form (Fig. 5d). The minimum of $R_{ss}$ is shifted towards the shorter wavelengths relative to the spike in the $R_{pp}$ spectrum.

With further increase of the angle $\varphi$, the $R_{pp}$ spectrum changes significantly. In particular, the spike vanishes, and the anomalous behavior in the region of the princi-

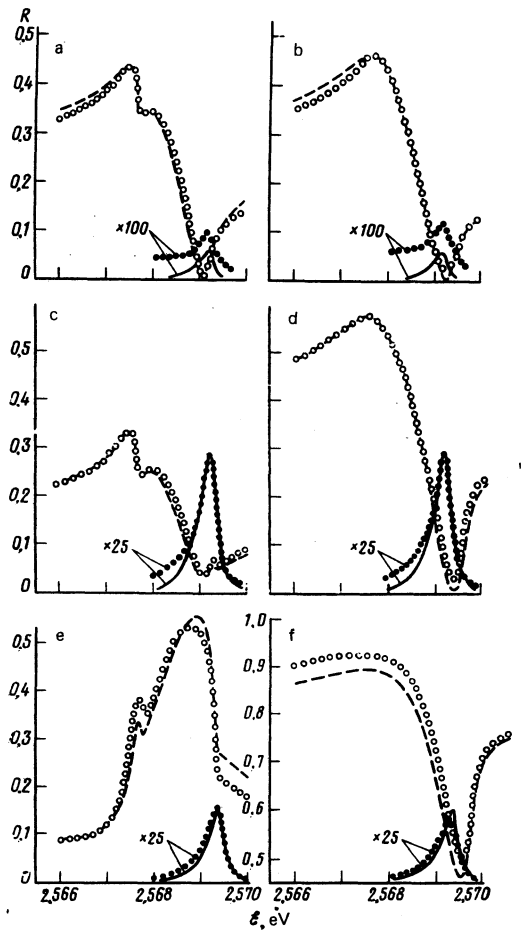


FIG. 5. Comparison of the experimental and theoretical reflection spectra $R_{pp}$, $R_{sp}$ (a, c, e) and $R_{ss}$, $R_{ps}$ (b, d, f) in the region of the exciton resonance $B_{n=1}$ at incidence angles $\varphi = 8°$ (a, b), 45° (c, d), 81.5° (e, f). The abscissa axis in Fig. 5f corresponds to the zero level of the $R_{ps}$ spectrum. ○—experimental $R_{pp}$ and $R_{ss}$ spectra, ●—experimental $R_{sp}$ and $R_{ps}$ spectra. Dashed—theoretical spectra $R_{pp}$ and $R_{ss}$, solid lines—theoretical spectra $R_{sp}$ and $R_{ps}$.

pal maximum is modified. Under conditions of "glancing" incidence ($\varphi = 81.5°$), the spectrum takes the form shown in Fig. 5e. The main characteristic feature of the $R_{ss}$ spectrum is a deep minimum (Fig. 5f).

As to the spectra obtained in orthogonal configurations of the polarizer and analyzer, they have a clearly pronounced resonant character. The spectral dependence of $R_{sp}$ or $R_{ps}$ is a narrow asymmetric peak located in the region of the principal minimum of the $R_{pp}$ spectrum. With decreasing incidence angle, the intensity of such a peak tends practically to zero (Fig. 5a and 5b). The background against which this peak is observed at $\varphi = 8°$ is due apparently to the diffuse component of the reflected light, which at such small incidence angle is already comparable with the specular orthogonal component. The coefficients $R_{ps}$ and $R_{sp}$ reach their maximum value (≈1%) near $\varphi = 45°$ (Fig. 5c and 5d) and decrease smoothly with increasing incidence angle from 50 to 85° (Figs. 5e and 5f). We note that in Fig. 5f the abscissa axis corresponds to the zero level in the $R_{ps}$ spectrum.

A comparison of the reflection spectra obtained in orthogonal configurations *ps* and *sp* shows that the intensity and shape of the reflection peaks of $R_{ps}$ and $R_{sp}$, at a fixed angle $\varphi$, practically coincide. Depending on the accuracy of the setting of the optical axis of the sample in the vertical direction, the intensities of these peaks and the ratio between them may vary. A criterion of a correct orientation of the crystal was the equality of the intensities $R_{ps}$ and $R_{sp}$ at $\varphi = 45°$ (see part I).

The $R_{ps}$ and $R_{sp}$ spectra shown in Figs. 5c and 5d differ somewhat in intensity from the analogous spectra of our preceding paper.[5] The reason is the less accurate procedure of determining the absolute values of the reflection coefficient and the insufficiently accurate orientation of the sample.[5]

We have dealt so far with reflection spectra in the region of the exciton resonance $B_{n=1}$. In the region of the exciton state $A_{n=1}$ the reflection spectra in the geometry of Fig. 2 are given for the *pp* configuration in Ref. 11. Our present measurements in the orthogonal configurations *ps* and *sp* have shown that the narrow peak of the $R_{ps}$ and $R_{sp}$ reflection is observed also in the region of the principal minimum of the $R_{pp}$ spectrum for the exciton *A*. This peak is similar in form to the corresponding peak in the region of the exciton *B*, but its intensity is weaker by almost one order of magnitude.

## 3. CHOICE OF PARAMETERS OF THE THEORY AND DISCUSSION OF THE RESULTS

According to the theory developed above, the optical properties of a crystal in the region of the exciton resonance $B_{n=1}$ and in the experimental geometry shown in Fig. 2 is characterized by a set of 17 parameters: $\omega_0$, $\omega_{LT}^{\perp}$, $\omega_{LT}^{\parallel}$, $M_\perp$, $\varepsilon_{0\parallel}$, $\varepsilon_{0\perp}$, $\Delta_1$, $\Delta_2$, $\beta_1$, $\beta_2$, $\alpha_\perp$, $\beta_\perp$, $\gamma_\parallel$, $l$, $\Gamma_\perp$, $\Gamma_\parallel$, and $\Gamma_Q$, where $\Gamma_\perp$, $\Gamma_\parallel$, and $\Gamma_Q$ are the damping parameters for the states $\Gamma_5$, $\Gamma_1$, and $\Gamma_2$, $\varkappa$ respectively, while $\Delta_1$ and $\Delta_2$ are the exchange constants (designated $\Delta_\parallel$ and $2\Delta_\perp$ in Ref. 9). By a suitable choice of these parameters it is possible to describe satisfactorily the entire set of the experimental spectra of Fig. 5, where the theoretical plots are shown dashed (the spectra $R_{pp}$ and $R_{ss}$) and solid (the spectra $R_{ps}$ and $R_{sp}$).

In the preliminary calculations, each of the parameters cited above was varied in a wide range, making it possible to establish the role of each of them in the formation of the reflection spectrum. It was then possible to ascertain which parameter is connected with any particular singularity of the spectrum. As result, despite the large number of parameter, their values could be chosen within narrow limits. These values were chosen primarily to be able to describe most accurately the experimental spectra at an incidence angle $\varphi = 45°$, inasmuch as at this angle the spectra have a large number of structural singularities and can be measured more accurately.

We now consider briefly the influence of each of the parameters on the form of the reflection spectra, and indicate their values chosen when the theoretical relations on Fig. 5 were calculated.

*Resonance frequency $\omega_0$ and the exchange constants $\Delta_1$ and $\Delta_2$.* Accurate to the values of the exchange constants, the resonance energy $\hbar\omega_0$ determined the spectral

positions of the reflection curves. The constants $\Delta_1$ and $\Delta_2$ lead to an additional shift of the spectra $R_{pp}$ and $R_{ss}$, including the shift relative to each other. The point of the spectrum $R_{pp}$ ($\varphi = 8°$; 45°) in the region of the singularity on the principal maximum, where the reflection curve has the largest slope relative to the abscissa axis, corresponds to the energy $\hbar\omega_0 - \Delta_1 - \Delta_2$. The positions of the peaks $R_{ps}$ and $R_{sp}$ and of the spike in the region of the principal minimum of the spectrum $R_{pp}(45°)$ are determined by the energy $\hbar(\omega_0 + \omega_{LT}^{\perp}) + \Delta_1$, while the minimum in the spectrum $R_{ss}(45°)$ corresponds approximately to the energies $\hbar(\omega_0 + \omega_{LT}^{\parallel}) - \Delta_1 + \Delta_2$. Using our measured positions of the distinct singularities of the spectra and comparing the shape and intensity of the theoretical and experimental reflection curves, we have obtained the following values of the parameters: $\hbar\omega_0 = 2567.65$ meV, $\Delta_1 = 0.01$ meV, and $\Delta_2 = -0.06$ meV.

*Longitudinal–transverse splittings $\omega_{LT}^{\perp}$ and $\omega_{LT}^{\parallel}$.* The values of $\omega_{LT}^{\perp}$ and $\omega_{LT}^{\parallel}$ determine in the main the spread of the spectra along the ordinate axis and the distance between the maximum and minimum in the $R_{pp}$ or $R_{ss}$ spectra: $\hbar\omega_{LT}^{\perp} = 1.58$ meV and $\hbar\omega_{LT}^{\parallel} = 1.94$ meV.

*Translational mass of the exciton $M_{\perp}$.* The value of $M_{\perp}$ determines the maximum values of the reflection coefficients in the configurations *pp* and *ss*, and also the appearance and form of the anomalies in the region of the principal minima. The value $M_{\perp} = 1.2\ m_0$ used by us agrees with the estimates of Mahan and Hopfield.[8]

*The phonon dielectric constants $\varepsilon_{0\perp}$ and $\varepsilon_{0\parallel}$.* The constants $\varepsilon_{0\perp}$ and $\varepsilon_{0\parallel}$ determine the values of the reflection coefficients $R_{pp}$ and $R_{ss}$ on the long- and short-wave sides of the structural parts of the spectra: $\varepsilon_{0\perp} = 10.2$; $\varepsilon_{0\parallel} = 10.0$.

*The constants $\beta_1$ and $\beta_2$ of the terms linear in* **k**. Since the NOA in the vicinity of the exciton resonance $B_{n=1}$ is connected with the constant $\beta_1$, the value of this constant determines the intensity of the reflection spectra in the orthogonal configurations *sp* and *ps*. When choosing the constant $\beta_1$ it must be borne in mind that the intensity of the half-width of the peak $R_{sp}$ or $R_{ps}$ depends also on the damping parameters $\Gamma_{\perp}$ and $\Gamma_{\parallel}$. The value $\beta_1\omega_0/c = -0.075$ meV makes it possible to account for the experimental result with sufficient accuracy.

The value of the constant $\beta_2$ influences the ratio of the reflection coefficients at the maximum of the spectrum $R_{pp}$ on the short-wave shoulder adjacent to this maximum. The sharpness of the structure depends on the parameters $\Gamma_{\perp}$ and $\Gamma_Q$. The theoretical curves in Fig. 5 were constructed at $\beta_2\omega_0/c = 0.06$ meV.

We note that the reflection spectra discussed in the present paper are not sensitive to the signs of the constants $\beta_1$ or $\beta_2$. The values $\beta_1 < 0$ and $\beta_2 > 0$ cited by us correspond to estimates[9] according to which $\beta_1 \approx -\beta_2$. It can be shown that the choice of the sign of the constant $\beta_1$ or $\beta_2$ fixes the direction of the polar axis of the crystal, and reversal of this sign is equivalent to change of the direction of the polar axis.[19] Our values of the constants $\beta_1$ and $\beta_2$ enable us to estimate the constant $\beta_3$ of the terms linear in **k** in the Hamiltonian of the exciton *A*. In fact, according to Ref. 9,

$$\beta_3 = \frac{1}{2}(\beta_1 + \beta_2)\frac{M_{\perp}^{B}}{M_{\perp}^{A}},$$

where $M_{\perp}^{A}$ and $M_{\perp}^{B} \equiv M_{\perp}$ are the translational masses of the excitons *A* and *B*. Using the values $M_{\perp}^{B} = 1.2\ m_0$ and $M_{\perp}^{A} = 0.9\ m_0$,[15] we get $\beta_3\omega_0/c = -0.01$ meV. This is much less than the values given above for $\beta_1$ and $\beta_2$. Therefore, in contrast to the exciton *B*, for the exciton *A* the terms linear in **k** do not lead to noticeable singularities in the reflection spectra $R_{pp}$.

*"Quadrupole" corrections to the matrix elements of the optical transition (the constants $\alpha_{\perp}$, $\beta_{\perp}$, and $\gamma_{\parallel}$).* Calculation has shown that the constants $\alpha_{\perp}$ and $\beta_{\perp}$ lead to qualitative and quantitative singularities which had not been observed in the experimental spectra of CdS. We have therefore put $\alpha_{\perp} = \beta_{\perp} = 0$. The correction connected with the constant $\gamma_{\parallel}$ makes a contribution of the NOA and its action on the $R_{ps}$ and $R_{sp}$ spectra is analogous to the action of the constant $\beta_1$. But to describe these spectra it is necessary to use such large values of $\gamma_{\parallel}$, that the theoretical spectra $R_{pp}$ and $R_{ss}$ lose their similarity to the experimentally observed spectra in the *pp* and *ss* configuration. It can therefore be assumed that $\gamma_{\parallel} = 0$.

It was already noted in the first part that the terms linear in **k** in the energy spectrum of the exciton $A_{n=1}$ do not lead to NOA. A contribution to the NOA can be made in this case by a quadrupole corrections similar to the correction with the constant $\gamma_{\parallel}$ for the exciton *B* [see Eq. (8)]. At $\gamma_{\parallel}^{A}\omega_0/c = 0.04$ we can satisfactorily duplicate the experimental spectrum $R_{ps}$ or $R_{sp}$ in the region of the exciton *A* without upsetting thereby the spectrum $R_{pp}$.

*Thickness $l$ of the transition layer.* When choosing the value of $l$ it must be borne in mind that in the experiment the spike produced by the transition layer appears in the $R_{pp}$ spectrum only if the incidence is oblique, and does not appear at all in the $R_{ss}$ spectrum (according to Fig. 3 parameter values are possible for which such a spike appears in each of the reflection spectra $R_{pp}$ and $R_{ss}$ at normal incidence). We note that variation of $l$ in the range from 0 to 120 Å does not influence substantially the spectra in the orthogonal configurations. We used in the calculation $l = 78$ Å.

*The damping parameters $\Gamma_{\perp}$, $\Gamma_{\parallel}$, and $\Gamma_Q$.* The values of these parameters influence mainly the accuracy of the reproduction of the additional structure in the reflection spectra. The quantity $\Gamma_Q$ characterized a section with additional structure in the region of the principal maximum of the $R_{pp}$ spectrum, while $\Gamma_{\perp}$ and $\Gamma_{\parallel}$ play a role in the spectral interval that includes the principal minima of the $R_{pp}$ and $R_{ss}$ spectra. On the remaining sections of the reflection spectra, such small values of the damping parameters have no significant effect. We have used the values $\hbar\Gamma_{\perp} = 0.185$ meV, $\hbar\Gamma_{\parallel} = 0.2$ meV, and $\hbar\Gamma_Q = 0.075$ meV.

The theoretical reflection spectra calculated using the foregoing values of the parameters of the exciton resonance $B_{n=1}$ in the CdS crystal and shown in Fig. 5 are in good agreement with the experimental data of the same figure. Some difference between the experimental and theoretical relations is apparently connected with the approximate character of the model of the transition layer,

and also with the fact that no account was taken in the calculation of the possible frequency dependence of the background dielectric constant and of the damping parameters within the limits of the reflection bands.

It was noted in the theoretical part that at $\beta_1 \neq 0$ there can be observed in the $R_{ss}$ spectrum, at the frequency of the principal minimum of the $R_{pp}$ spectrum (energy $\mathscr{E}_L^{\perp}$), an additional singularity in the form of a local minimum (Fig. 3b, dashed curve). However, in the reflection spectra of the CdS crystals this singularity, which is due to NOA, does not appear. Nor is it seen on the theoretical curves of Fig. 5. The reason is that in the CdS crystals the additional singularity lands in the region of the principal minimum of the $R_{ss}$ spectrum, and does not come into view. It was of interest to investigate the reflection spectra of such crystals with wurtzite structures, in which the longitudinal–transverse splittings $\omega_{LT}^{\parallel}$ and $\omega_{LT}^{\perp}$ differ strongly and the minima of the $R_{pp}$ and $R_{ss}$ spectra are noticeably separated. Such crystals include the $\beta$ modification of AgI, whose reflection spectra are given in Ref. 6. In accord with the theoretical predictions, a local minimum was observed in the $R_{ss}$ spectrum of the AgI crystal at the frequency of the principal minimum of the $R_{pp}$ spectrum. A numerical calculation[6] within the framework of the theory developed above agrees well with the experimental data. We note that methodological difficulties prevented the authors of Ref. 6 to register the characteristic reflection peaks in orthogonal configurations.

We have thus investigated in this paper, theoretically and experimentally, a group of phenomena connected with a unique manifestation of NOA of crystals with wurtzite structure. The agreement between the results of the theory and of the experiments attest to the applicability of the theory developed here to a description of the NOA of crystals of symmetry $C_{3v}$, $C_{4v}$ and $C_{6v}$ in the region of the frequencies of the excitonic resonances.

In conclusion, the authors thank G. E. Pikus and S. A. Permogorov for suggesting the considered questions and for interest in the work, and V. M. Agranovich for a helpful discussion.

[1]V. M. Agranovich and V. L. Ginzburg, Kristallooptika s uchetom prostranstvennoĭ dispersii i teorii eksitonov (Spatial Dispersion in Crystal Optics and Exciton Theory), Nauka, 1965 [Wiley, 1966].
[2]V. A. Kizel', Yu. I. Krasilov, and V. I. Burkov, Usp. Fiz. Nauk **114**, 295 (1974) [Sov. Phys. Usp. **17**, 745 (1975)].
[3]F. I. Fedorov, Opt. Spektrosk. **6**, 377 (1959); F. I. Fedorov, B. V. Bokut', and A. F. Konstantinova, Kristallografiya **7**, 910 (1962) [Sov. Phys. Crystallogr. **7**, 738 (1963)].
[4]B. V. Bokut' and A. N. Serdyukov, Zh. Eksp. Teor. Fiz. **61**, 1808 (1971) [Sov. Phys. JETP **34**, 962 (1972)].
[5]E. L. Ivchenko, S. A. Permogorov, and A. V. Sel'kin, Pis'ma Zh. Eksp. Teor. Fiz. **27**, 27 (1978) [JETP Lett. **27**, 24 (1978)].
[6]T. M. Mashlyatina, D. S. Nedzvetskiĭ, and A. V. Sel'kin, Pis'ma Zh. Eksp. Teor. Fiz. **27**, 573 (1978) [JETP Lett. **27**, 539 (1978)].
[7]E. I. Rashba and V. I. Sheka, Fiz. Tverd. Tela (Leningrad) **1**, 162 (1959) [Sov. Phys. Solid State **1**, 143 (1959)].
[8]G. D. Mahan and J. J. Hopfield, Phys. Rev. **135**, A 428 (1964).
[9]G. E. Pikus and G. L. Bir, Fiz. Tekh. Poluprovodn. **7**, 119 (1973) [Sov. Phys. Semicond. **7**, 81 (1973)].
[10]S. I. Pekar, Zh. Eksp. Teor. Fiz. **33**, 1022 (1957) [Sov. Phys. JETP **6**, 785 (1958)].
[11]S. A. Permogorov, V. V. Travnikov, and A. V. Sel'kin, Fiz. Tverd. Tela (Leningrad) **14**, 3646 (1972); **15**, 1822 (1973) [Sov. Phys. Solid State **14**, (1973); **15**, 1215 (1973)].
[12]V. A. Kiselev, B. S. Razbirin, and I. N. Ural'tsev, Pis'ma Zh. Eksp. Teor. Fiz. **18**, 504 (1973) [JETP Lett. **18**, 296 (1973)].
[13]R. Zeyher, J. L. Birman, and W. Brenig, Phys. Rev. **B6**, 4613 (1972).
[14]O. V. Konstantinov, M. M. Panakhov, and Sh. R. Saĭfullaev, Fiz. Tverd. Tela (Leningrad) **17**, 3551 (1975) [Sov. Phys. Solid State **17**, 2315 (1975)].
[15]J. J. Hopfield and D. G. Thomas, Phys. Rev. **132**, 563 (1963).
[16]A. V. Sel'kin, Phys. Status Solidi **B83**, 47 (1977).
[17]V. M. Agranovich and V. I. Yudson, Opt. Commun. **5**, 422 (1972; **9**, 58 (1973).
[18]L. E. Solov'ev and V. S. Rudakov, Vestn. Leningr. Univ. Fiz. Khim. **4**, 23 (1968).
[19]E. L. Ivchenko, S. A. Permogorov, and A. V. Sel'kin, Pis'ma Zh. Eksp. Teor. Fiz. **28**, 649 (1978) [JETP Lett. **28**, 599 (1978)].

Translated by J. G. Adashko